

Original Article

Combretastatin A4 disodium phosphate-induced myocardial injury

Ryota Tochinai^{1*}, Yuriiko Nagata¹, Minoru Ando¹, Chie Hata¹, Tomo Suzuki¹, Naoyuki Asakawa¹, Kazuhiko Yoshizawa¹, Kazumi Uchida¹, Shoichi Kado¹, Toshihide Kobayashi¹, Kimiyuki Kaneko¹, and Masayoshi Kuwahara²

¹ Yakult Central Institute, Yakult Honsha Co., Ltd., 5-11 Izumi, Kunitachi-shi, Tokyo 186-8650, Japan

² Department of Veterinary Pathophysiology and Animal Health, Graduate School of Agricultural and Life Sciences, The University of Tokyo, 1-1-1 Yayoi, Bunkyo-ku, Tokyo 113-8657, Japan

Abstract: Histopathological and electrocardiographic features of myocardial lesions induced by combretastatin A4 disodium phosphate (CA4DP) were evaluated, and the relation between myocardial lesions and vascular changes and the direct toxic effect of CA4DP on cardiomyocytes were discussed. We induced myocardial lesions by administration of CA4DP to rats and evaluated myocardial damage by histopathologic examination and electrocardiography. We evaluated blood pressure (BP) of CA4DP-treated rats and effects of CA4DP on cellular impedance-based contractility of human induced pluripotent stem cell-derived cardiomyocytes (hiPS-CMs). The results revealed multifocal myocardial necrosis with a predilection for the interventricular septum and subendocardial regions of the apex of the left ventricular wall, injury of capillaries, morphological change of the ST junction, and QT interval prolongation. The histopathological profile of myocardial lesions suggested that CA4DP induced a lack of myocardial blood flow. CA4DP increased the diastolic BP and showed direct effects on hiPS-CMs. These results suggest that CA4DP induces dysfunction of small arteries and capillaries and has direct toxicity in cardiomyocytes. Therefore, it is thought that CA4DP induced capillary and myocardial injury due to collapse of the microcirculation in the myocardium. Moreover, the direct toxic effect of CA4DP on cardiomyocytes induced myocardial lesions in a coordinated manner. (DOI: 10.1293/tox.2016-0012; J Toxicol Pathol 2016; 29: 163–171)

Key words: combretastatin A4, fosbretabulin, cardiotoxicity, blood pressure, cardiac necrosis, capillary

Introduction

Combretastatin A4 disodium phosphate (CA4DP; fosbretabulin) [*cis*-1-(3,4,5-trimethoxy-phenyl)-2-(4'-methoxyphenyl) ethane-3'-0-phosphate, disodium salt] is the prodrug of the tubulin-disassembling agent combretastatin A4 (CA4) derived from *Combretum caffrum*¹. Preclinical studies have demonstrated that CA4DP inhibits tumor vascularization and induces central tumor necrosis^{2, 3}. However, whereas therapeutic benefits of CA4DP were found in clinical trials, hypertension, tachycardia, bradycardia, QT prolongation, and myocardial infarction were observed at a high frequency⁴. This cardiovascular toxicity of CA4DP is a major risk of chemotherapy, because CA4DP tends to be administered to older patients who have co-existing cardiovascular disease.

Microtubules play roles in cardiac development and the regulation of contraction⁵. It has already been reported that a high dose of microtubule-disassembling agents such as colchicine and vincristine induced myocardial damage in rats^{6–8}, whereas a low dose of these drugs had cardioprotective effects^{9, 10}. As for CA4DP, the hypertensive effect of CA4DP and inhibitory effect of antihypertensive drugs have been studied¹¹. Also, electrocardiogram (ECG) evidence of an acute coronary syndrome was observed in a clinical trial¹². Therefore, it is thought that a change in vascular function is involved in cardiac damage. However, the histopathological profile of myocardial lesions and the underlying mechanism of cardiotoxicity induced by CA4DP are not known, and the relation between the vascular change and myocardial lesions has not been fully discussed. In addition, it is presumed that CA4DP affects potential repolarization in the ventricular myocardium¹². Moreover, several *in vitro* studies have revealed that colchicine, another microtubule-disassembling agent, stimulates beating cardiomyocytes¹³ and enhances Na⁺ and Ca²⁺ currents in cardiomyocytes^{5, 14, 15}. However, laboratory evidence about the direct effects of CA4DP on cardiomyocytes has not been reported.

This study aimed to clarify the histopathological and electrocardiographic features of myocardial lesions induced by CA4DP and to discuss the relation between myocardial

Received: 10 February 2016, Accepted: 6 April 2016

Published online in J-STAGE: 23 April 2016

*Corresponding Author: R Tochinai

(e-mail: ryota-tochinai@yakult.co.jp)

©2016 The Japanese Society of Toxicologic Pathology

This is an open-access article distributed under the terms of the Creative Commons Attribution Non-Commercial No Derivatives (by-nc-nd) License <<http://creativecommons.org/licenses/by-nc-nd/4.0/>>.

Table 1. Group Design of the Histopathological Evaluation

	Test article			
	Saline 10 mL/kg 2 times 72 h interval	CA4DP 30 mg/10 mL/kg 4 times 24 h intervals	CA4DP 60 mg/10 mL/kg 4 times 24 h intervals	CA4DP 120 mg/10 mL/kg 2 times 72 h interval
Number of animals	5	2	2*	5

*One rat died after the last administration

lesions and vascular change and the direct toxic effect on cardiomyocytes. First, we made an attempt to induce myocardial lesions by administration of CA4DP to healthy rats and evaluated myocardial damage histopathologically and electrocardiographically. Next, in order to examine the relation between myocardial lesions and vascular change, we evaluated blood pressure (BP) in CA4DP-treated rats. Moreover, the effect of CA4DP on cellular impedance-based contractility (an *in vitro* measure of cell viability and contractility^{16–20}) was evaluated using human induced pluripotent stem cell-derived cardiomyocytes (hiPS-CMs), in order to examine the direct effect of CA4DP on cardiomyocytes.

Materials and Methods

Ethics

All experiments using rats were conducted in accordance with the guidance of the Institutional Animal Care and Use Committee of Yakult Central Institute or the Animal Experimentation Guidelines of the University of Tokyo, and were approved by the Institutional Animal Care and Use Committee of Yakult Central Institute or the Institutional Animal Care and Use Committee of the Graduate School of Agricultural and Life Sciences at the University of Tokyo. All experiments using hiPS-CMs were approved by the Human Studies Committee of Yakult Central Institute, Tokyo, Japan, in accordance with the guidelines of the Helsinki Declaration and the Human Studies Committee.

Animals

Male SD rats (CrI:CD(SD)) aged 5–6 weeks were used. Rats were singly-housed in plastic or stainless steel mesh cages in a controlled environment (light-dark cycle 12/12 hours, temperature $23 \pm 3^\circ\text{C}$) with ad libitum access to laboratory basal feed and tap water.

Chemicals

CA4DP was purchased from MedKoo Biosciences (Chapel Hill, NC, USA) and Sigma-Aldrich (St. Louis, MO, USA). CA4 was obtained from Sigma-Aldrich.

Evaluation of histopathological changes

A total of 14 rats were divided into four groups as described in Table 1. At 6 weeks of age, CA4DP (four doses of 30 or 60 mg/10 mL/kg at intervals of 24 hours or two doses of 120 mg/10 mL/kg at an interval of 72 hours) or saline

(two doses at an interval of 72 hours) was administered via the caudal vein by bolus infusion. On the day after the last administration, the rats were anesthetized with isoflurane, and necropsy was performed. Also, one rat administered four doses of CA4DP 60 mg/10 mL/kg died unexpectedly before necropsy because of CA4DP toxicity. The cause of death was thought to be the cardiotoxicity of CA4DP because severe myocardial necrosis had been observed in this rat. After exsanguination, the hearts of the rats were removed and immediately fixed in 10% neutral phosphate-buffered formalin. The fixed hearts were cross-sectioned in two planes through the ventricles as described in a previous report⁷. The fixed hearts were embedded in paraffin and sectioned at a thickness of 4–6 μm . The specimens were stained with hematoxylin and eosin (HE). Observation of these specimens was performed using a light microscope (BX51, Olympus Corporation, Tokyo, Japan).

Evaluation of ECG data

Two rats were used (animal No. 1 and No. 2). At 5 weeks of age, a small telemetry device (weight = 3.9 g, volume = 1.9 cc; TA10ETA-F20, Data Sciences International, New Brighton, MN, USA) for transmitting ECG data was implanted in the dorsal subcutaneous region under anesthesia with pentobarbital sodium. Paired wire electrodes that came with the telemetry device were placed under the skin of the dorsal and ventral thorax to record the apex-base (A–B) lead ECG. One week after surgery, ECG signals were recorded from each rat in a cage that had been placed on a signal-receiving board (RA1610, Data Sciences International, New Brighton, MN, USA). ECG data were continuously sampled at 1 ms intervals, and all data analyses of ECG-wave components were performed using an ECG processor analyzing system (SRV2W and SP-2000, Softron, Tokyo, Japan) on a personal computer in series with an analog-digital converter; the ECG data were stored on an external hard disk. During the period of ECG recording, CA4DP 50 mg/10 mL/kg was administered to both rats via the caudal vein by bolus infusion, 3 times at intervals of 24 hours. ECG was recorded until 12 hours after the third administration. The consecutive ECG waves for 4 seconds were averaged, and the ECG wave components (RR interval, QRS duration, PR interval, and QT interval) were analyzed.

Evaluation of BP

A total of 9 rats were used. At 6 weeks of age, rats were anesthetized with isoflurane, and placed in a supine position. The femoral artery was exposed, and a polyethylene catheter filled with heparinized saline was inserted. The catheter was connected to transducer amplification equipment (Nippon Denki San-ei, Tokyo, Japan) via a pressure transducer (Nihon Kohden Corporation, Tokyo, Japan), and the arterial pressure was recorded. BP was continuously sampled at 1 ms intervals, and all data analyses were performed using an ECG processor analyzing system (SBP-2000, Softron, Tokyo, Japan) on a personal computer in series with an analog-digital converter. During the period of BP recording, CA4DP 120 mg/10 mL/kg or saline 10 mL/kg was administered as a single dose via the caudal vein by bolus infusion ($n = 5$ for CA4DP and $n = 4$ for saline). BP was recorded until 30 minutes after administration. Consecutive BP waves for 4 seconds were averaged, and the BP components (systolic BP [SBP], diastolic BP [DBP], and mean BP [MBP]) and heart rate (HR) were analyzed.

Toxicokinetic analysis

Rats were administered a single intravenous dose of CA4DP at 120 mg/10 mL/kg by bolus infusion ($n = 3$). Blood was taken via the jugular vein and collected in heparin-coated tubes at 10 minutes and 1, 3, 6, and 24 hours after administration. Plasma was separated by centrifugation immediately after sampling. After centrifugation, an aliquot of plasma was mixed with the equivalent volume of 1% formic acid and stored at -20°C . The thawed plasma samples were purified by solid-phase extraction, and the plasma concentrations of combretastatin A4 phosphate (free base of CA4DP; CA4P) and combretastatin A4 (the metabolite of CA4DP; CA4) were determined by liquid chromatography-tandem mass spectrometry (LC-MS/MS). Toxicokinetic parameters [maximum concentration (C_{\max}), terminal half-life ($T_{1/2}$), and area under the concentration-time curve from time zero to infinity ($\text{AUC}_{0-\infty}$)] were obtained by non-compartmental analysis using Phoenix WinNonlin 6.3 (Certara USA, Inc., Princeton, NJ, USA).

Evaluation of cellular impedance

Analysis of cellular impedance of hiPS-CMs using an xCELLigence Cardio Analyzer (ACEA Biosciences, San Diego, CA, USA) was performed with reference to and modification of the methods in earlier studies^{16–20}. Briefly, iCell hiPS-CMs were purchased from Cellular Dynamics International (Madison, WI, USA). hiPS-CMs were thawed and cultured in 96-well xCELLigence Cardio E-plates (ACEA Biosciences) at 20,000 cells/well and 37°C in 5% CO_2 , using plating medium and maintenance medium specifically for iCell hiPS-CMs (Cellular Dynamics International), according to the manufacturer's protocol. During the incubation period, the impedance values^{19, 20} were monitored continuously using an xCELLigence Cardio Analyzer according to the manufacturer's instructions. Impedance was continuously sampled at 12.9 ms intervals and monitored at every

measurement point with a 20 second sweep duration. After incubation for 14 days, test compounds (100 nM, 1 μM , and 10 μM CA4DP; 100 nM, 1 μM , and 10 μM CA4; and 0.1% H_2O for CA4DP or 0.1% DMSO for CA4 [vehicle]) ($n = 3$ well) were added to the culture. Then, impedance cell index (CI)^{17, 19, 20} and beating rate^{16, 18, 20} were calculated using dedicated software. Data for CI and beating rate were normalized by the value immediately before the addition of test compounds. The CI for 36 hours after administration was used to detect cytotoxic effects. The beating rate at 15 minutes, 3 hours, and 12 hours after administration were used to detect changes in contractility.

Statistics

Mann-Whitney's U-test was used for analysis of blood pressure. Dunnett's test was used for analysis of beating rate using cellular impedance.

Results

Evaluation of histopathological changes

In the ventricles of rats given four doses of CA4DP at 30 mg/10 mL/kg at intervals of 24 hours, infiltration of inflammatory cells around capillaries was observed (Fig. 1A). In the ventricles of the rat given four doses of CA4DP at 60 mg/10 mL/kg at intervals of 24 hours (the surviving rat), edema around capillaries and pyknosis of capillary endothelial cells (Fig. 1B) were observed. On the other hand, relatively larger arteries in the heart did not show obvious change in these rats. In the ventricles of rats given four doses of CA4DP at 60 mg/10 mL/kg at intervals of 24 hours (the rat that died) or two doses of CA4DP at 120 mg/10 mL/kg at an interval of 72 hours, multifocal necrosis of the myocardium, infiltration of inflammatory cells, and dilatation of capillaries (Fig. 1C) were observed. Sites of predilection for these myocardial lesions were the interventricular septum and subendocardial regions of the apex of the left ventricular wall (Fig. 1D).

Evaluation of ECG data

The ST junction became obvious after the second administration of CA4DP 50 mg/10 mL/kg (Fig. 2B). The RR interval and PR interval at 1–3 hours after the second and third administrations became longer than those at right before administration (Fig. 3A, C). Therefore, it was thought that the RR interval and PR interval were transiently prolonged at 1–3 hours after the second and third administrations (Fig. 3A, C). The QT interval on the day before administration showed little variation; however, it gradually became prolonged throughout the dosing period (Fig. 3D). This prolongation of the QT interval was irrespective of the change in RR interval (Fig. 3E). The QRS duration was not altered during the dosing period (Fig. 3B).

Evaluation of BP

DBP and MBP at 30 minutes after administration were higher in rats treated with CA4DP 120 mg/10 mL/

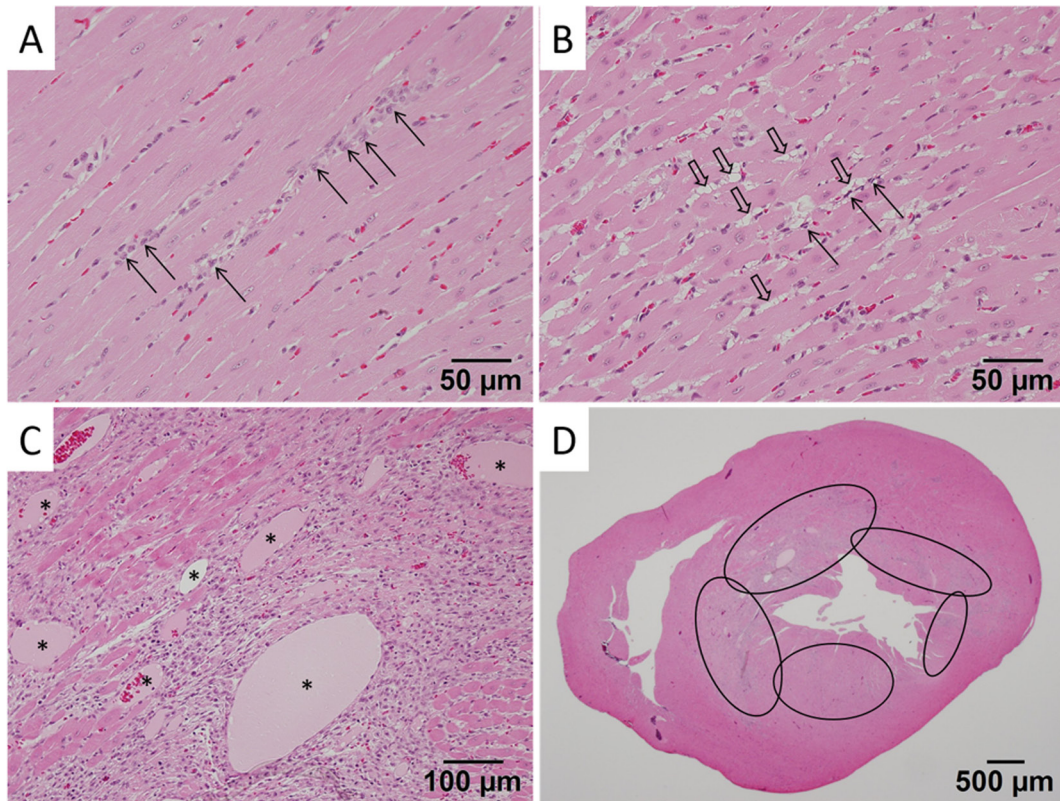


Fig. 1. Micrographs of myocardial lesions in rats administered CA4DP. A: Infiltration of inflammatory cells (arrows) around capillaries in the ventricle of a rat given four doses of CA4DP 30 mg/10 mL/kg at intervals of 24 h. B: Edema (open arrows) around capillaries and pyknosis of capillary endothelial cells (linear arrows) in the ventricle of a surviving rat given four doses of CA4DP 60 mg/10 mL/kg at intervals of 24 h. C: Multifocal necrosis of the myocardium, infiltration of inflammatory cells, and dilatation of capillaries (*) in the ventricle of a rat given two doses of CA4DP 120 mg/10 mL/kg at an interval of 72 h. D: Site of predilection of myocardial lesions induced by two doses of CA4DP 120 mg/10 mL/kg at an interval of 72 h. Myocardial lesions were prominent in the interventricular septum and subendocardial regions of the apex of the left ventricular wall (ellipses).

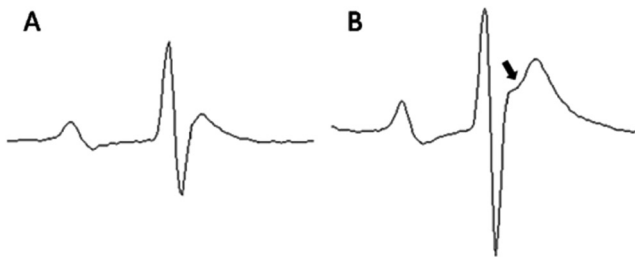


Fig. 2. Representative averaged ECG traces before (A) and after (B) administration of CA4DP. A: Normal ECG of a rat before administration of CA4DP. The ST junction is not obvious. B: ECG of a rat after administration of CA4DP 50 mg/10 mL/kg. This trace was obtained 23 hours after the second administration of CA4DP 50 mg/10 mL/kg. In this ECG, the ST junction is obvious (arrow).

kg (Fig. 4A, C, D). On the other hand, SBP did not change for 30 minutes in rats treated with CA4DP 120 mg/10 mL/kg (Fig. 4B). HR slightly decreased at 5 minutes after administration in rats treated with CA4DP 120 mg/10 mL/kg (Fig. 4E).

Toxicokinetic analysis

The toxicokinetic parameters of CA4P and CA4 in rats treated with CA4DP 120 mg/10 mL/kg are indicated in Table 2. The values of C_{max} , $T_{1/2}$, and AUC_{0-inf} for CA4P were $298 \pm 39 \mu\text{M}$, $0.868 \pm 0.044 \text{ h}$, and $153 \pm 24 \text{ h}\cdot\mu\text{M}$, respectively. Those for CA4 were $156 \pm 13 \mu\text{M}$, $5.87 \pm 1.69 \text{ h}$, and $89.4 \pm 10.1 \text{ h}\cdot\mu\text{M}$, respectively.

Evaluation of cellular impedance

The CI of the CA4DP-treated hiPS-CMs rapidly decreased by 5–10% within 1 hour. Moreover, from 4–5 hours after administration, the CI began to decrease gradually, and it continued to do so for the remainder of the recording period (Fig. 5A). The CI of the CA4-treated hiPS-CMs decreased in a manner similar to CA4DP-treated hiPS-CMs (Fig. 5B).

The beating rate of the CA4DP-treated hiPS-CMs was increased at 3 hours and 24 hours after administration (Fig. 6A). The beating rate of the CA4-treated hiPS-CMs was increased at 15 minutes, 3 hours, and 24 hours after administration (Fig. 6B).

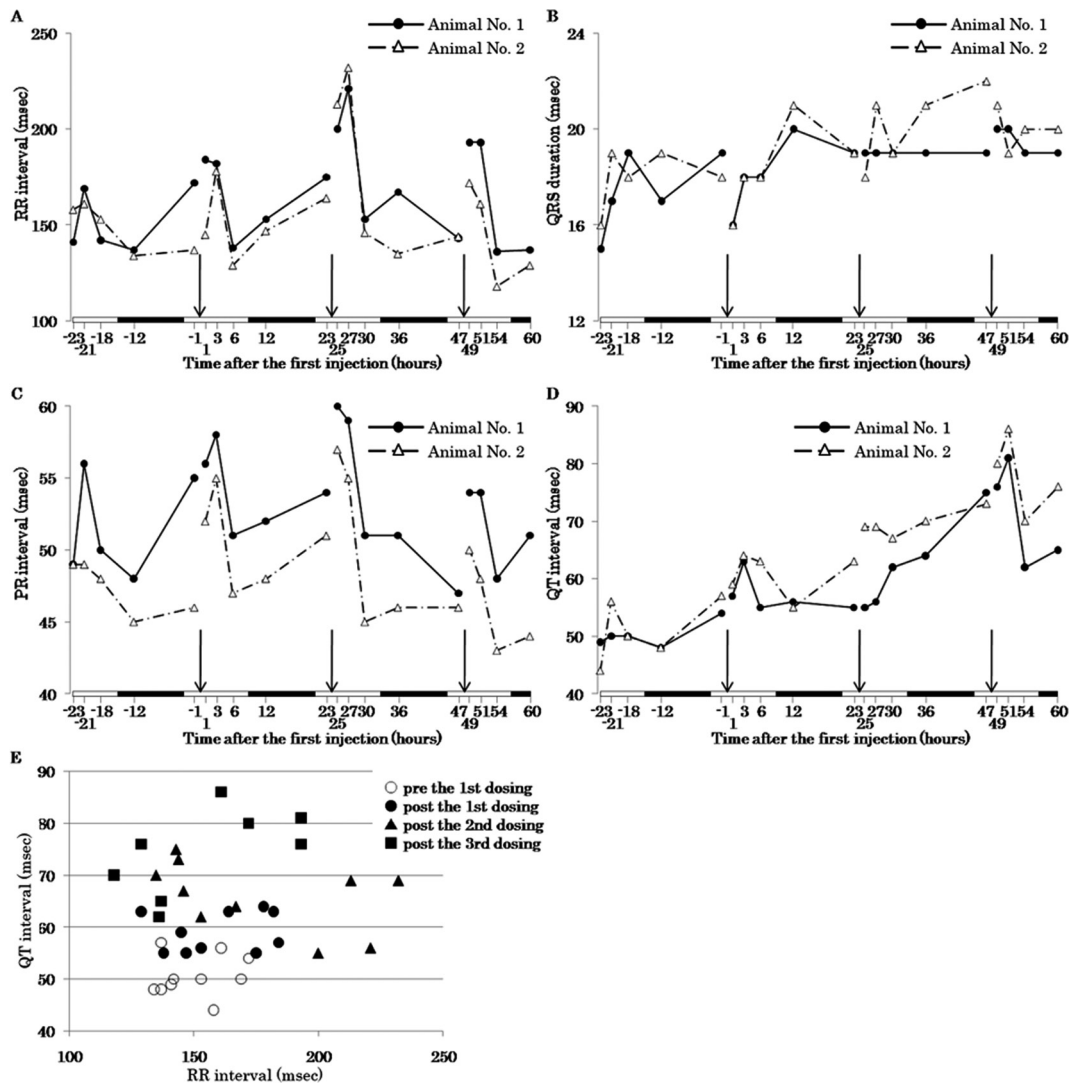


Fig. 3. Time-response curves of the RR interval (A), QRS duration (B), PR interval (C), QT interval (D), and QT-RR plot (E) before and after administration of CA4DP. A–D: The solid line indicates the result of animal No. 1, and the dashed line indicates the result of animal No. 2. Both animal No. 1 and No. 2 were administered CA4DP 50 mg/10 mL/kg. Arrows indicate time points of administration of CA4DP. White bars and filled bars in horizontal axes indicate the light period and dark period, respectively. A: The RR interval was prolonged at 1–3 hours after the second and subsequent administration. B: The QRS duration was not altered during the dosing period. C: The PR interval was prolonged at 1–3 hours after the second and subsequent administration. D: The QT interval was gradually prolonged throughout the dosing period. E: The QT interval was prolonged after administration of CA4DP irrespective of changes in the RR interval.

Discussion

In our histopathological analysis, multifocal myocardial necrosis was observed in the interventricular septum and inner layer of the apex of the left ventricular wall. It is generally thought that the myocardium of the interventricular septum and inner layer of the apex of the left ventricular wall develops multifocal necrosis when regional blood flow becomes low relative to the workload of the myocardium. So, it is thought that CA4DP induced a regional lack of blood flow in the heart of the rats. In addition, histopathological changes of capillary endothelial cells of the heart were induced by CA4DP. Therefore, it seems reasonable to

suppose that CA4DP induced microcirculatory collapse in the myocardium and that this microcirculatory collapse led to a decrease in blood supply and injury of the myocardium. Our previous report suggested that other microtubule-disassembling agents (colchicine and vincristine) induce hypoxia of the myocardium along with vascular endothelial damage⁷. However, CA4DP is used as an inhibitor of tumor vascularization, and it has been revealed that overdose of CA4DP injures vascular endothelial cells of normal tissue, as in the case of other microtubule-disassembling agents.

We detected myocardial changes induced by CA4DP not only by histopathological analysis but also by ECG analysis. Whereas rats are not suitable for prediction of the

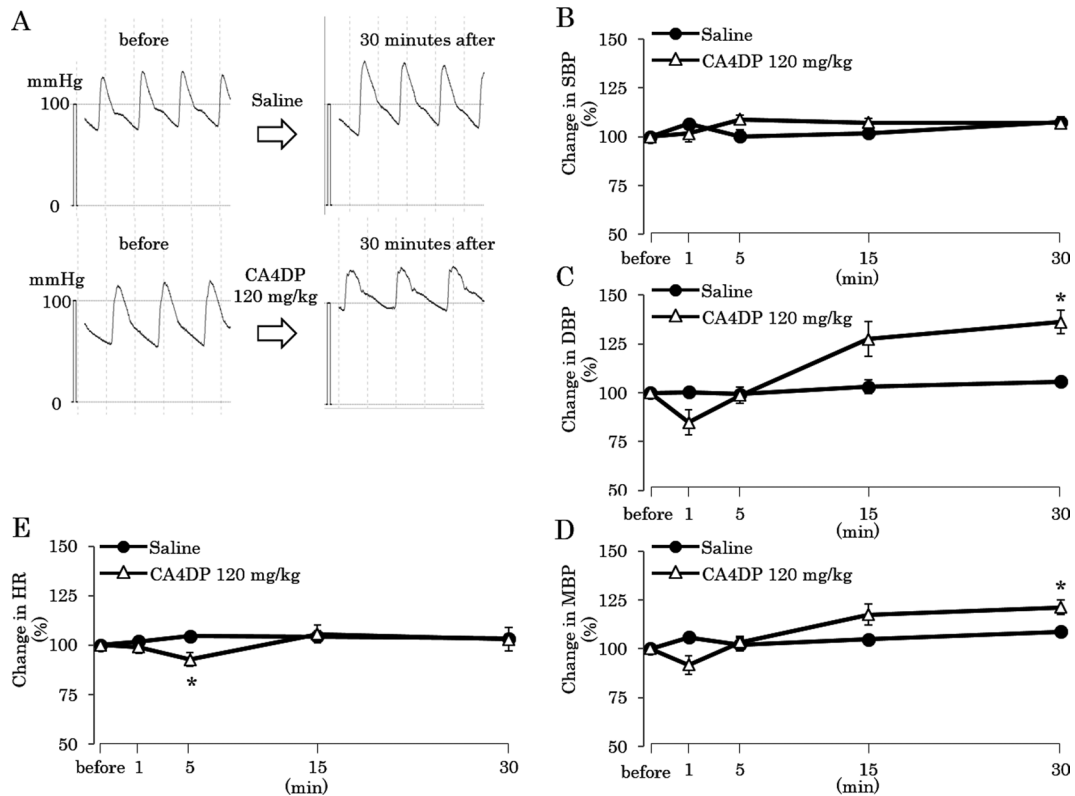


Fig. 4. Time-response curves of BP of rats given CA4DP or saline. A: Blood pressure tracings in rats given CA4DP 120 mg/10 mL/kg or saline 10 mL/kg. B: Time course of SBP change in response to a single intravenous injection of CA4DP 120 mg/10 mL/kg or saline 10 mL/kg. The SBP of CA4DP-treated rats did not change throughout the recording period. C: Time course of DBP change in response to a single intravenous injection of CA4DP 120 mg/10 mL/kg or saline 10 mL/kg. The DBP of CA4DP-treated rats became higher than that of saline 10 mL/kg-treated rats at 30 minutes after administration. D: Time course of MBP change in response to a single intravenous injection of CA4DP 120 mg/10 mL/kg or saline 10 mL/kg. The MBP of CA4DP-treated rats became higher than that of saline 10 mL/kg-treated rats at 30 minutes after administration. E: Time course of HR change in response to a single intravenous injection of CA4DP 120 mg/10 mL/kg or saline 10 mL/kg. The HR of CA4DP 120 mg/10 mL/kg-treated rats decreased slightly at 5 minutes after administration. B–E: Each dot represents a mean \pm SE. *: $p < 0.05$ compared with rats given saline.

Table 2. The Toxicokinetic Behavior of CA4P and CA4 in CA4DP 120 mg/10 mL/kg-treated Rats

Dose	Analyte	C_{max} (μ M)	$T_{1/2}$ (h)	AUC_{0-inf} (h \cdot μ M)
CA4DP	CA4P	298 \pm 39	0.868 \pm 0.044	153 \pm 24
120 mg/10 mL/kg	CA4	156 \pm 13	5.87 \pm 1.69	89.4 \pm 10.1

risk of torsade de pointes because their dominant transient outward current relies on the transient outward K^+ current (IKto), multiple studies have shown the similarity of pathophysiological changes in the ECG of rats and humans²¹. Therefore, it has been claimed that rat ECG analysis has utility in toxicology. In CA4DP-treated rats, the morphological features of the ST junction was altered, and the QT interval was prolonged. It is thought that the QT prolongation observed in this study can be explained by a secondary change following ST junction alteration induced by myocardial damage. Myocardial damage in the interventricular septum and inner layer of the apex of the left ventricular wall may be the cause of morphological change of the ST junction.

We also evaluated the change in BP induced by CA4DP in order to discuss the relation between myocardial lesions and vascular change. BP analysis showed that administration of CA4DP for 30 minutes induced an increase only in DBP but not in SBP. Conventionally, it has been assumed that high vascular resistance, which is produced by small arteries and capillaries, is reflected by an elevated DBP, whereas the SBP is determined by the stroke volume and compliance of larger arteries²². Therefore, the most likely explanation for the CA4DP-induced BP change is that small arteries and capillaries became less elastic due to the effects of CA4DP but that larger arteries did not change at that time. Since endothelial cells play an important role in regulation of vascular tension by production of vasoactive agents such

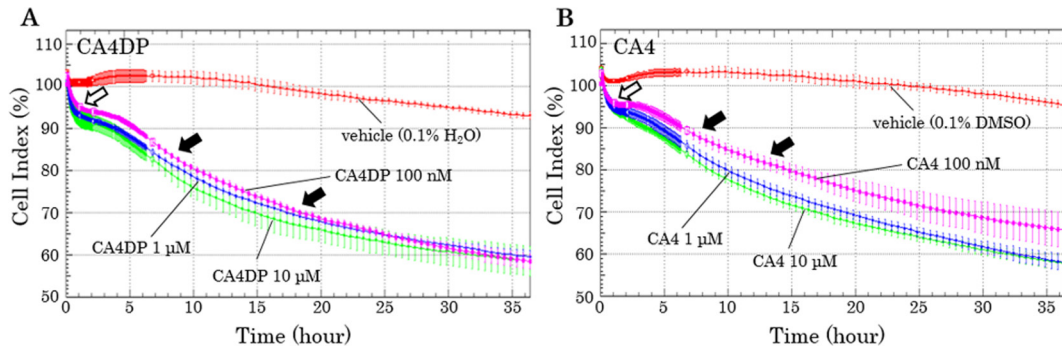


Fig. 5. Time-response curves of the cell index (CI) of hiPS-CMs given CA4DP, CA4, or vehicle. A: Time course of CI change in response to administration of CA4DP or vehicle (0.1% H₂O). B: Time course of CI change in response to administration of CA4 or vehicle (0.1% DMSO). A, B: The CIs of CA4DP-treated hiPS-CMs and CA4-treated hiPS-CMs decreased rapidly within 1 hour (white arrow). From 4–5 hours after administration, the CI began to decrease gradually, and it continued to do so for the remainder of the recording period (black arrows). A, B: Each dot represents a mean \pm SD.

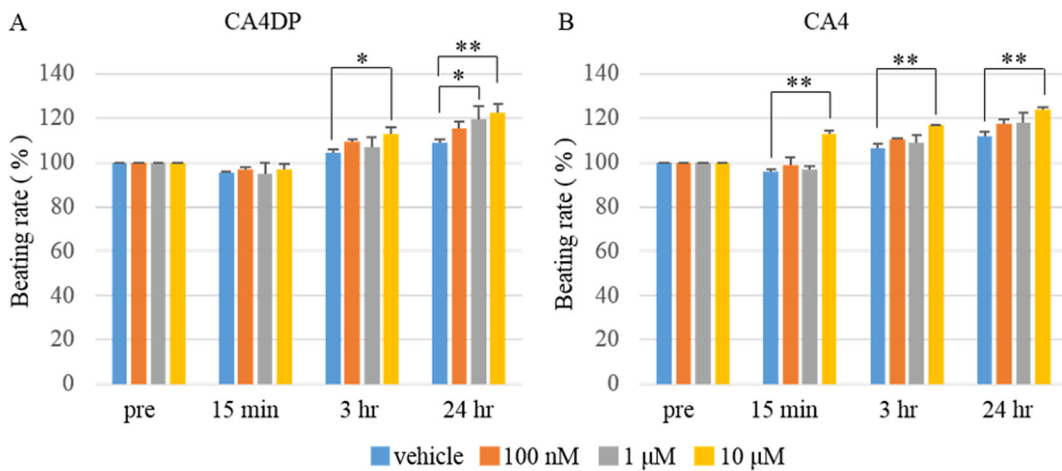


Fig. 6. Change of beating rate of hiPS-CMs in response to administration of CA4DP, CA4, or vehicle. A: Change of beating rate in response to administration of CA4DP or vehicle (0.1% H₂O). The beating rate of hiPS-CMs was increased at 3 hours and 12 hours after administration of CA4DP. B: Change of beating rate in response to administration of CA4 or vehicle (0.1% DMSO). The beating rate of hiPS-CMs was increased at 15 minutes, 3 hours, and 12 hours after administration of CA4. A, B: Each dot represents a mean \pm SD. * p <0.05 compared with hiPS-CMs given vehicle; ** p <0.01 compared with hiPS-CMs given vehicle.

as endothelin and nitric oxide^{23, 24}, endothelial damage induced by CA4DP may be related to hypertensive effects. Further studies are needed to clarify the molecular mechanism of the hypertensive effect of CA4DP. Moreover, it is reported that endothelial microtubule disruption blocked flow-mediated dilation of arterioles of the heart and skeletal muscle²⁵. This loss of elasticity of small arteries and capillaries and inhibition of dilation of arterioles may be exacerbative causes of the lack of blood flow in the heart.

Finally, we used hiPS-CMs to examine the possibility that CA4DP and CA4 (the metabolic product of CA4DP) have direct toxicity in cardiomyocytes. hiPS-CMs have major ion channels, receptors, transporters, and contractile proteins and are known to respond to selective modulators in a manner similar to the human myocardium^{20, 26–28}. Therefore, it is thought that hiPS-CMs are useful for predic-

tion of cardiotoxicity in clinical situations. We administered CA4DP and CA4 at 100 nM–10 μ M to hiPS-CMs. This concentration range is thought to be suitable for experimental conditions, since the values of C_{max} for CA4P and CA4 were higher than 10 μ M. In this study, we evaluated the cellular impedance-based contractility of hiPS-CMs, a newly proposed *in vitro* measure of cell viability and contractility^{16–20}. It is reported that alteration of cell morphology induces a rapid change in CI and that decrease of the live cell number induces a decrease in CI over a prolonged timescale¹⁹. The results of this study showed that CA4DP and CA4 induced a biphasic response resulting in a decrease in CI: a rapid decrease within 1 hour and a slow decrease throughout the rest of the recording period. It was considered that the rapid decrease of the CI indicates alteration of the morphology of the hiPS-CMs by disruption of the cytoskeleton and that

the slow decrease of the CI indicates loss of live hiPS-CMs due to the cytotoxicity of CA4DP and CA4 in addition to alteration of the morphology of the hiPS-CMs. Moreover, the beating rate of the hiPS-CMs treated with CA4DP and CA4 increased. These results suggest that CA4DP and CA4 have cardiostimulatory activity. These direct effects of CA4DP and CA4 on cardiomyocytes may be a cause of myocardial damage. In an earlier report, it was revealed that tubulin-disassembling agents, such as colchicine, nocodazole, and vincristine, enhanced beating of cardiomyocytes isolated from newborn rats¹³. CA4DP may have the same cardiostimulatory mechanism as other tubulin-disassembling agents. It has been proposed that microtubules degrade the sarcomeric performance of cardiomyocytes by imposing a viscous load on the cytoplasm^{29, 30} and regulate the activates of Na⁺ channels and Ca²⁺ channels in cardiomyocytes^{5, 14, 15}. These molecular mechanisms may be involved in the increase in the beating rate of cardiomyocytes. The detailed mechanism by which these microtubule-disassembling agents stimulate cardiomyocytes remains to be elucidated. Meanwhile, the RR interval was not shortened in *in vivo* ECG analysis. In *in vivo* ECG analysis, the RR interval and PR interval of CA4DP-treated rats became prolonged. Therefore, it is thought that parasympathetic nervous activity was increased in CA4DP-treated rats. It is likely that a vicarious increase in parasympathetic nervous activity occurred in response to BP elevation and that this increase in parasympathetic nervous activity masked the cardiostimulatory activities of CA4DP and CA4. However, these direct effects of CA4DP on cardiomyocytes may be only part of the cause of cardiotoxicity, because myocardial lesions *in vivo* were not diffuse but instead were multifocal with a predilection for the interventricular septum and subendocardial regions of the apex of the left ventricular wall. It is considered that collapse of the microcirculation and direct cytotoxicity may act in concert to damage the myocardium.

In conclusion, we demonstrated that CA4DP induced myocardial lesions in healthy rats, which were suggested to be the result of a regional lack of blood flow, in addition to myocardial capillary lesions. Moreover, CA4DP induced morphological alteration of the ST junction with prolongation of the QT interval and an increase in DBP. Microcirculatory collapse due to endothelial damage was suggested to be the main cause of the CA4DP-induced regional lack of blood flow. In addition, CA4DP showed a direct toxic effect on cardiomyocytes. This direct toxic effect on cardiomyocytes and dysfunction of myocardial capillaries presumably caused myocardial lesions in a coordinated manner. Based on our results, it is speculated that control of blood pressure and protection of capillary endothelial cells are important for prevention of the cardiotoxicity of CA4DP. Further integrated studies with molecular and whole-body approaches under controlled blood pressure and endothelial cell conditions are needed to better understand coping strategies for the cardiotoxicity of CA4DP.

Disclosure of Potential Conflicts of Interest: The authors declare that they have no conflicts of interest.

References

1. Pettit GR, Cragg GM, Herald DL, Schmidt JM, and Lohavanijaya P. Isolation and structure of combretastatin. *Can J Chem.* **60**: 1374–1376. 1982. [[CrossRef](#)]
2. Dark GG, Hill SA, Prise VE, Tozer GM, Pettit GR, and Chaplin DJ. Combretastatin A-4, an agent that displays potent and selective toxicity toward tumor vasculature. *Cancer Res.* **57**: 1829–1834. 1997. [[Medline](#)]
3. Tozer GM, Prise VE, Wilson J, Locke RJ, Vojnovic B, Stratford MR, Dennis MF, and Chaplin DJ. Combretastatin A-4 phosphate as a tumor vascular-targeting agent: early effects in tumors and normal tissues. *Cancer Res.* **59**: 1626–1634. 1999. [[Medline](#)]
4. Subbiah IM, Lenihan DJ, and Tsimberidou AM. Cardiovascular toxicity profiles of vascular-disrupting agents. *Oncologist.* **16**: 1120–1130. 2011. [[Medline](#)] [[CrossRef](#)]
5. Webster DR. Microtubules in cardiac toxicity and disease. *Cardiovasc Toxicol.* **2**: 75–89. 2002. [[Medline](#)] [[CrossRef](#)]
6. Mikaelian I, Buness A, de Vera-Mudry MC, Kanwal C, Coluccio D, Rasmussen E, Char HW, Carvajal V, Hilton H, Funk J, Hofflack JC, Fielden M, Herting F, Dunn M, and Suter-Dick L. Primary endothelial damage is the mechanism of cardiotoxicity of tubulin-binding drugs. *Toxicol Sci.* **117**: 144–151. 2010. [[Medline](#)] [[CrossRef](#)]
7. Tochinai R, Ando M, Suzuki T, Suzuki K, Nagata Y, Hata C, Uchida K, Kobayashi T, Kado S, and Kaneko K. Histopathological studies of microtubule disassembling agent-induced myocardial lesions in rats. *Exp Toxicol Pathol.* **65**: 737–743. 2013. [[Medline](#)] [[CrossRef](#)]
8. Tochinai R, Suzuki K, Nagata Y, Ando M, Hata C, Komatsu K, Suzuki T, Uchida K, Kado S, Kaneko K, and Kuwahara M. Cardiotoxic changes of colchicine intoxication in rats: electrocardiographic, histopathological and blood chemical analysis. *J Toxicol Pathol.* **27**: 223–230. 2014. [[Medline](#)] [[CrossRef](#)]
9. Verma S, Eikelboom JW, Nidorf SM, Al-Omran M, Gupta N, Teoh H, and Friedrich JO. Colchicine in cardiac disease: a systematic review and meta-analysis of randomized controlled trials. *BMC Cardiovasc Disord.* **15**: 96. 2015. [[Medline](#)] [[CrossRef](#)]
10. Panda S, and Kar A. Combined Effects of Vincristine and Quercetin in Reducing Isoproterenol-Induced Cardiac Necrosis in Rats. *Cardiovasc Toxicol.* **15**: 291–299. 2015. [[Medline](#)] [[CrossRef](#)]
11. Ke Q, Bodyak N, Rigor DL, Hurst NW, Chaplin DJ, and Kang PM. Pharmacological inhibition of the hypertensive response to combretastatin A-4 phosphate in rats. *Vascul Pharmacol.* **51**: 337–343. 2009. [[Medline](#)] [[CrossRef](#)]
12. Cooney MM, Radivoyevitch T, Dowlati A, Overmoyer B, Levitan N, Robertson K, Levine SL, DeCaro K, Buchter C, Taylor A, Stambler BS, and Remick SC. Cardiovascular safety profile of combretastatin A4 phosphate in a single-dose phase I study in patients with advanced cancer. *Clin Cancer Res.* **10**: 96–100. 2004. [[Medline](#)] [[CrossRef](#)]
13. Lampidis TJ, Kolonias D, Savaraj N, and Rubin RW. Cardiostimulatory and antiarrhythmic activity of tubulin-bind-

- ing agents. *Proc Natl Acad Sci USA*. **89**: 1256–1260. 1992. [[Medline](#)] [[CrossRef](#)]
14. Gómez AM, Kerfant BG, and Vassort G. Microtubule disruption modulates Ca(2+) signaling in rat cardiac myocytes. *Circ Res*. **86**: 30–36. 2000. [[Medline](#)] [[CrossRef](#)]
 15. Motlagh D, Alden KJ, Russell B, and García J. Sodium current modulation by a tubulin/GTP coupled process in rat neonatal cardiac myocytes. *J Physiol*. **540**: 93–103. 2002. [[Medline](#)] [[CrossRef](#)]
 16. Guo L, Abrams RM, Babiarz JE, Cohen JD, Kameoka S, Sanders MJ, Chiao E, and Kolaja KL. Estimating the risk of drug-induced proarrhythmia using human induced pluripotent stem cell-derived cardiomyocytes. *Toxicol Sci*. **123**: 281–289. 2011. [[Medline](#)] [[CrossRef](#)]
 17. Kustermann S, Boess F, Buness A, Schmitz M, Watzele M, Weiser T, Singer T, Suter L, and Roth A. A label-free, impedance-based real time assay to identify drug-induced toxicities and differentiate cytostatic from cytotoxic effects. *Toxicol In Vitro*. **27**: 1589–1595. 2013. [[Medline](#)] [[CrossRef](#)]
 18. Guo L, Eldridge S, Furniss M, Mussio J, and Davis M. Use of human induced pluripotent stem cell-derived cardiomyocytes (hiPSC-CMs) to monitor compound effects on cardiac myocyte signaling pathway. *Curr Protoc Chem Biol*. **7**: 141–185. 2015. [[Medline](#)] [[CrossRef](#)]
 19. Denelavas A, Weibel F, Prummer M, Imbach A, Clerc RG, Apfel CM, and Hertel C. Real-time cellular impedance measurements detect Ca²⁺ channel-dependent oscillations of morphology in human H295R adrenoma cells. *Biochim Biophys Acta*. **1813**: 754–762. 2011. [[Medline](#)] [[CrossRef](#)]
 20. Guo L, Coyle L, Abrams RMC, Kemper R, Chiao ET, and Kolaja KL. Refining the human iPSC-cardiomyocyte arrhythmic risk assessment model. *Toxicol Sci*. **136**: 581–594. 2013. [[Medline](#)] [[CrossRef](#)]
 21. Farraj AK, Hazari MS, and Cascio WE. The utility of the small rodent electrocardiogram in toxicology. *Toxicol Sci*. **121**: 11–30. 2011. [[Medline](#)] [[CrossRef](#)]
 22. Galarza CR, Alfie J, Waisman GD, Mayorga LM, Cámara LA, del Río M, Vasvari F, Limansky R, Fariás J, Tessler J, and Cámara MI. Diastolic pressure underestimates age-related hemodynamic impairment. *Hypertension*. **30**: 809–816. 1997. [[Medline](#)] [[CrossRef](#)]
 23. Gibbons GH. Endothelial function as a determinant of vascular function and structure: a new therapeutic target. *Am J Cardiol*. **79**(5A): 3–8. 1997. [[Medline](#)] [[CrossRef](#)]
 24. Malek AM, Lee IW, Alper SL, and Izumo S. Regulation of endothelin-1 gene expression by cell shape and the microfilament network in vascular endothelium. *Am J Physiol*. **273**: C1764–C1774. 1997. [[Medline](#)]
 25. Liu Y, Li H, Bubolz AH, Zhang DX, and Gutterman DD. Endothelial cytoskeletal elements are critical for flow-mediated dilation in human coronary arterioles. *Med Biol Eng Comput*. **46**: 469–478. 2008. [[Medline](#)] [[CrossRef](#)]
 26. Khan JM, Lyon AR, and Harding SE. The case for induced pluripotent stem cell-derived cardiomyocytes in pharmacological screening. *Br J Pharmacol*. **169**: 304–317. 2013. [[Medline](#)] [[CrossRef](#)]
 27. Babiarz JE, Ravon M, Sridhar S, Ravindran P, Swanson B, Bitter H, Weiser T, Chiao E, Certa U, and Kolaja KL. Determination of the human cardiomyocyte mRNA and miRNA differentiation network by fine-scale profiling. *Stem Cells Dev*. **21**: 1956–1965. 2012. [[Medline](#)] [[CrossRef](#)]
 28. Ma J, Guo L, Fiene SJ, Anson BD, Thomson JA, Kamp TJ, Kolaja KL, Swanson BJ, and January CT. High purity human-induced pluripotent stem cell-derived cardiomyocytes: electrophysiological properties of action potentials and ionic currents. *Am J Physiol Heart Circ Physiol*. **301**: H2006–H2017. 2011. [[Medline](#)] [[CrossRef](#)]
 29. Tagawa H, Wang N, Narishige T, Ingber DE, Zile MR, and Cooper G 4th. Cytoskeletal mechanics in pressure-overload cardiac hypertrophy. *Circ Res*. **80**: 281–289. 1997. [[Medline](#)] [[CrossRef](#)]
 30. Webster DR, and Patrick DL. Beating rate of isolated neonatal cardiomyocytes is regulated by the stable microtubule subset. *Am J Physiol Heart Circ Physiol*. **278**: H1653–H1661. 2000. [[Medline](#)]